

The Afterglows and Host Galaxies of Short GRBs: An Overview

Edo Berger

Carnegie Observatories, Pasadena, CA

Abstract. Despite a rich diversity in observational properties, gamma-ray bursts (GRBs) can be divided into two broad categories based on their duration and spectral hardness – the long-soft and the short-hard GRBs. The discovery of afterglows from long GRBs in 1997, and their localization to arcsecond accuracy, was a watershed event. The ensuing decade of intense study led to the realization that long-soft GRBs are located in star forming galaxies, produce about 10^{51} erg in collimated relativistic ejecta, are accompanied by supernovae, and result from the death of massive stars. While theoretical arguments suggest that short GRBs have a different physical origin, the lack of detectable afterglows prevented definitive conclusions. The situation changed dramatically starting in May 2005 with the discovery of the first afterglows from short GRBs localized by *Swift* and *HETE-2*. Here I summarize the discovery of these afterglows and the underlying host galaxies, and draw initial conclusions about the nature of the progenitors and the properties of the bursts.

HISTORY AND MODELS

The detection of short-duration gamma-ray bursts (GRBs) dates back to the *Vela* satellites [1]. However, only in 1993 the short bursts (with $T_{90} \lesssim 2$ s) were recognized as a separate sub-class from the long GRBs, and were furthermore shown to have on average a harder γ -ray spectrum [2]; hereafter I will refer to short-hard bursts as SHBs. The short durations of SHBs suggest that they are unlikely to result from the death of massive stars, for which the natural timescale (the free-fall time) is significantly longer, $t_{ff} \approx 30\text{ s} (M/10M_\odot)^{-1/2} (R/10^{10}\text{ cm})^{3/2}$.

Instead the main theoretical thrust has been focused on coalescing compact objects – neutron stars and/or black holes (DNS or NS-BH) – as the progenitors of SHBs [3, 4, 5, 6, 7]. In this context the duration, which is set by the viscous timescale of the gas accreting onto the newly-formed black hole, is short due to the small scale of the system. Other progenitors have been proposed in addition to the DNS and NS-BH systems, namely magnetars, thought to be the power source behind soft γ -ray repeaters [8], and accretion-induced collapse (AIC) of neutron stars [9, 10]. The magnetar model is unlikely to account for SHBs at cosmological distances, since even the 2004 Dec. 27 giant flare from SGR 1806-20 would only be detected by *BATSE* or *Swift* at $\lesssim 50$ Mpc; magnetars may contribute to a local population of SHBs. The AIC model has not been investigated in detail, but in the case of a white dwarf was shown to be too baryon rich to produce GRBs [11].

Naturally, without a distance and energy scale, or an understanding of the micro- and macro-environments of SHBs, it is nearly impossible to make any quantitative statements about their progenitors or the detailed underlying physics. As in the case of

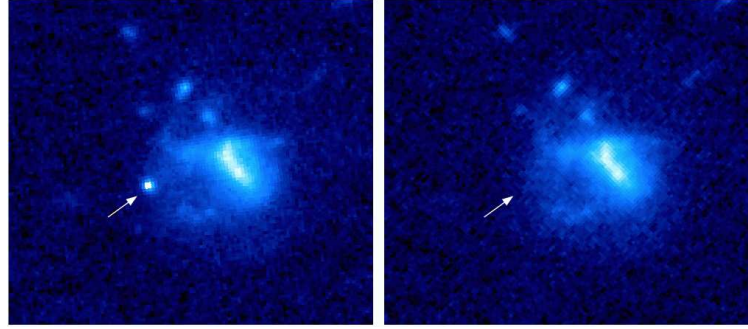


FIGURE 1. HST images of the optical afterglow and irregular star forming host of GRB 050709.

the long GRBs, this understanding relies on arcsecond positions, which in turn require the identification of afterglows. Several SHBs have been localized to sufficient accuracy (few arcmin²) in the past to allow afterglow searches, but none have been detected at optical or radio wavelengths due to delayed and shallow searches [12].

THE DISCOVERY OF SHORT GRB AFTERGLOWS

The breakthrough in understanding the origin and properties of SHBs resulted from the localization of the first afterglows starting in May 2005. Here I provide a short account of these discoveries, highlighting the growing understanding achieved with each burst.

GRB 050509b was detected by *Swift* on 2005 May 9.167 UT with a duration of 40 ms and a fluence, $F_\gamma = 9.5 \times 10^{-9}$ erg cm⁻² [13]. A fading X-ray afterglow was localized with the XRT onboard *Swift* to a positional accuracy of 9.3'' radius [13]. Despite intense follow-up at optical and radio wavelengths no candidates were discovered to a limit of 24 mag at $t \approx 2.5$ hr [14, 15] and 0.1 mJy at $t \approx 2.2$ hr [16], respectively. Instead, a bright elliptical galaxy ($L \approx 3L^*$) at $z = 0.225$ was detected in coincidence with the X-ray error circle [14, 13]. The *a posteriori* probability of such a coincidence has been estimated at 0.01 – 1% [14, 13, 17]. The implication of this possible association is that the progenitors of SHBs are related to an old stellar population. Unfortunately, the XRT error circle also contains over twenty fainter galaxies, which most likely reside at higher redshifts, thereby preventing a definitive association. The optical follow-up also placed a limit of $M_B > -13.3$ mag (5 mag fainter than SN 1998bw) on a supernova coincident with GRB 050509b [14, 15], providing additional support to a non-massive star origin *if the redshift of $z = 0.225$ is adopted*.

GRB 050709 was detected by *HETE-2* on May 9.942 UT with a duration of 70 ms and a fluence, 4.0×10^{-7} erg cm⁻² (2 – 400 keV). The initial pulse was followed 25 s later by a softer X-ray bump with a duration of 130 s and a fluence of 1.1×10^{-6} erg cm⁻² (2 – 25 keV) [19]. Observations with *Chandra* provided an arcsecond position [20], and led to the discovery of the optical afterglow [21, 20] (Fig. 1). No radio afterglow was detected [20]. Spectroscopy revealed that the host is a star forming galaxy at $z = 0.160$, but HST imaging showed that the burst did not coincide with a bright star forming region [20]. No

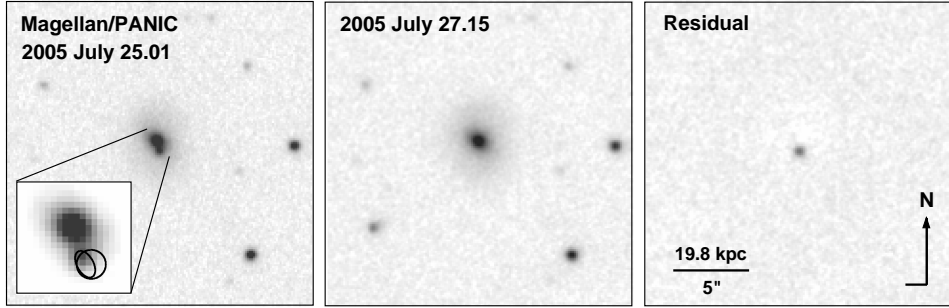


FIGURE 2. Magellan near-IR images of the afterglow and host galaxy of GRB 050724 on two separate occasions, and the residual image clearly showing the fading afterglow. The inset shows the radio (ellipse) and X-ray (circle) positions of the afterglow. From Ref. [18].

supernova component was detected [21]. These results suggest that while GRB 050709 occurred in a star forming galaxy, it was not related to a massive star.

GRB 050724 was localized by *Swift* on 2005 July 24.524 UT with a duration of 3 ± 1 s, dominated by an initial spike of 250 ms duration, and a fluence, $F_\gamma = 3.9 \times 10^{-7}$ erg cm^{-2} (15 – 150 keV) [22]. As in the case of GRB 050709, the initial pulse was followed 30 s later by a soft bump (15 – 25 keV) which lasted 120 s, but with a fluence of only 10% that of the main pulse. A bright X-ray afterglow detected by XRT [22] led to the discovery of the radio, optical and near-IR afterglow, which coincided with a bright elliptical galaxy at $z = 0.257$ (Fig. 2) [18]. This burst provided the first unambiguous association with a galaxy undergoing no current star formation; the limit at the position of the GRB is $< 0.05 \text{ M}_\odot \text{ yr}^{-1}$ [18]. The X-ray and optical light curves revealed a broad increase by nearly an order of magnitude at 0.65 d, suggestive of energy injection [22, 18]. The subsequent steep decline at $t \gtrsim 1$ d is reminiscent of the jet breaks detected in long GRBs, indicating a jet opening angle of about 8.5° [18].

GRB 050813 was detected by *Swift* on 2005 August 13.281 UT with a duration of 0.6 s and a fluence, 4.3×10^{-8} erg cm^{-2} (15 – 150 keV). The initial X-ray position included a pair of galaxies, of which one is at a redshift $z = 0.72$ [23, 24], and appears to be part of a galaxy cluster [25]. However, the revised XRT position excludes these galaxies, and instead contains a galaxy at $z \approx 1.8$, which appears to be part of a cluster at that redshift. No optical or radio afterglows were detected. Since this is the highest redshift SHB to date, it has significant implications for the progenitor lifetime (see below).

GRB 051221 is perhaps the best-studied SHB to date. It was discovered by *Swift* on 2005 December 21.077 with an initial hard pulse of 250 ms duration, followed by softer emission, which lasted about 1 s, and a total fluence, 3.2×10^{-6} erg cm^{-2} (20 – 2000 keV) [27, 28]. The X-ray afterglow was localized to $3.5''$ radius accuracy [29], leading to the identification of the optical, near-IR, and radio counterparts [26] (Fig. 3). A spectrum of the combined afterglow and host indicated a redshift of $z = 0.546$ [26]. The afterglow evolution follows a simple power law decay to $t \approx 13$ d, interrupted only by a period of flattening from 1.4 to 3.1 hr in the X-rays and reverse shock emission in the radio band (Fig. 4). The light curve evolution indicates an opening angle $> 13^\circ$, an energy injection of about a factor of three, and a total energy of at least 1.0×10^{50} erg [26].

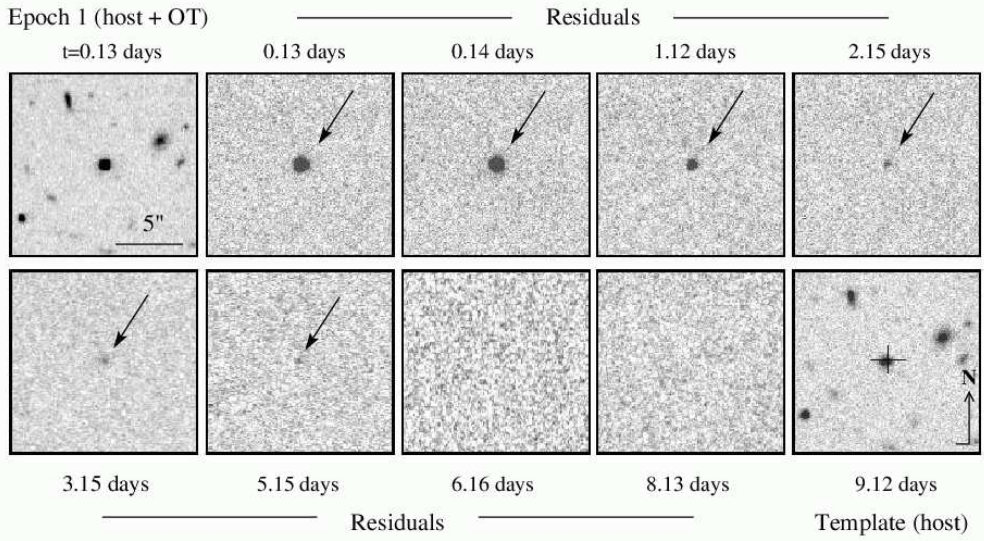


FIGURE 3. The fading optical afterglow and host galaxy of GRB 051221. From Ref. [26].

THE PROPERTIES AND PROGENITORS OF SHORT GRBS

The discovery of SHB afterglows allows us to address for the first time the basic questions regarding the nature and properties of these events:

- What is the energy release of SHBs (prompt emission and relativistic blast wave)?
- Is there evidence for prolonged engine activity?
- Are the ejecta collimated or spherical?
- Are SHBs accompanied by supernova-like events?
- What is the density and structure of the circumburst medium?
- In what type of host galaxies do SHBs occur?

Short GRB Energetics

The redshift distribution of the five SHBs with precise or putative redshifts ranges from about 0.16 to ~ 1.8 , with three of the five bursts at $z \lesssim 0.3$ (Fig. 5); GRB 050813 stands out with a significantly higher redshift. At the same time, a statistical comparison of BATSE SHB positions to low-redshift galaxy catalogs suggests that $\sim 10 - 25\%$ of the BATSE SHBs may originate within 100 Mpc [30]. The isotropic γ -ray energies span a wide range, $E_{\gamma,\text{iso}} \approx 1.1 \times 10^{48} - 3 \times 10^{51}$ erg, which is at the low end of the distribution for long GRBs (Fig. 5) [20]. The afterglow X-ray luminosities, which serve as a proxy for the blast-wave kinetic energy [31], span an equally wide range, $L_{X,\text{iso}}(t = 10\text{ hr}) \approx 7.0 \times 10^{41} - 6.4 \times 10^{44}$ erg s^{-1} . These values are again at the low end of the distribution for long GRBs [32].

As in the case of long GRBs, the true energy release is strongly dependent on collimation of the ejecta. Both GRBs 050709 and 050724 exhibit evidence for jets through

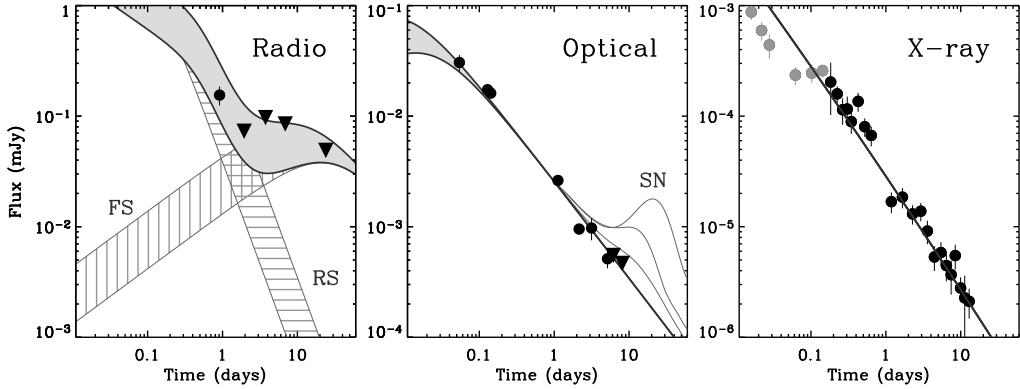


FIGURE 4. Broad-band light curves of the afterglow of GRB 051221. The black lines and shaded regions are model fits, which include forward shock emission and the reverse shock contribution in the radio, which is associated with the energy injection episode in the X-rays (at 0.05 d). From Ref. [26].

breaks and steep decays of their afterglow light curves [18, 20]. In the former case the opening angle is 14° while for the latter it is about 8.5° . GRB 051221, on the other hand, exhibits no clear break out to at least 13 days, or $\theta_j > 13^\circ$ [26]. The inferred jet angles are consistently wider than the median value of $\langle \theta_j \rangle \approx 5^\circ$ for long GRBs [26].

The broad-band light curves of GRBs 050709, 050724, and 051221 also allow a rough determination of the blast wave kinetic energies using the standard synchrotron model [33, 26] (Fig. 4). The parameters of interest are E_{KE} , the circumburst density (n), and the fractions of energy in relativistic electron (ϵ_e) and magnetic fields (ϵ_B). The values derived for the three SHBs are summarized in Tab. 1, and the derived beaming corrected energies are plotted in Fig. 5 [18, 20, 26]. The energies of GRBs 050709 and 050724 are about two orders of magnitude lower than those of long GRBs, $E \approx \text{few} \times 10^{51} \text{ erg}$ [34, 35, 36], but GRB 051221 has an energy that is at least an order of magnitude larger, and potentially as large as that of long GRBs.

The energy scale of GRB 051221 has important implications for the energy extraction mechanism, $\nu\bar{\nu}$ annihilation or MHD processes related to the black hole and/or the accretion disk [37, 7]. Numerical calculations reveal that $\nu\bar{\nu}$ annihilation is unlikely to power an SHB with a beaming-corrected energy in excess of $\text{few} \times 10^{48} \text{ erg}$, while MHD processes can produce $> 10^{52} \text{ erg s}^{-1}$. Thus, GRBs 050709 and 050724 could in principle be powered by $\nu\bar{\nu}$ annihilation, but it is unlikely that GRB 051221 was [26].

Prolonged Engine Activity

One of the intriguing results emerging from observations of the prompt emission and X-ray afterglows is evidence for prolonged engine activity and delayed energy injection. A hint of this result was already available from summed light curves of BATSE SHBs, which led to the possible detection of excess emission peaking ~ 30 s after the burst with a duration of ~ 100 s [38, 39]. This was originally proposed as evidence for afterglow emission, but there is now evidence from GRBs 050709 and 050724 that this is not the

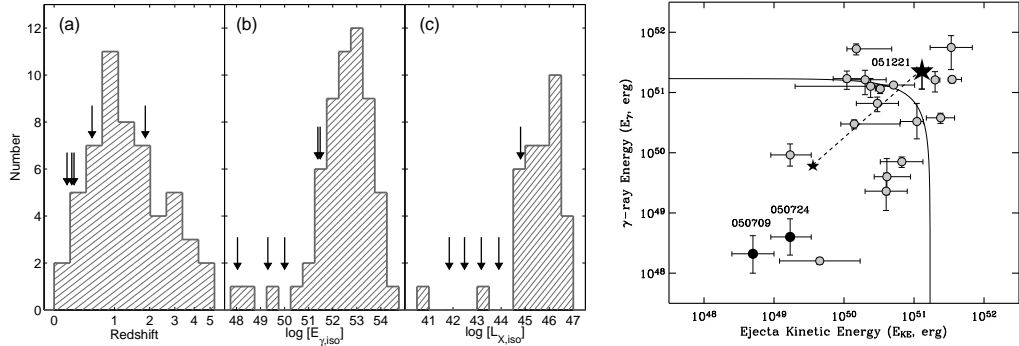


FIGURE 5. *Left:* Distributions of (a) redshift, (b) isotropic γ -ray energy, and (c) isotropic X-ray luminosity (a proxy for the blast wave kinetic energy). Adapted from Ref. [20]. *Right:* Beaming corrected γ -ray and afterglow kinetic energies for SHBs (black) and long GRBs (gray). From Ref. [26].

TABLE 1. Physical Properties of SHBs

	050709	050724	051221
Redshift	0.160	0.257	0.546
$E_{\gamma, \text{iso}}$ (erg)	6.9×10^{49}	4.0×10^{50}	2.4×10^{51}
$E_{\text{KE,iso}}$ (erg)	1.6×10^{48}	1.5×10^{51}	1.4×10^{51}
n (cm $^{-3}$)	~ 0.01	~ 0.1	$\sim 10^{-3}$
ϵ_e	~ 0.3	~ 0.04	~ 0.3
ϵ_B	~ 0.3	~ 0.02	~ 0.1
θ_j (deg)	14	9	> 13
f_b	0.03	0.01	> 0.03
E_{γ} (erg)	2.1×10^{48}	4.5×10^{48}	$(6 - 240) \times 10^{49}$
E_{KE} (erg)	5.0×10^{48}	1.7×10^{49}	$(4 - 140) \times 10^{49}$
Reference	[20]	[18]	[26]

case (Fig. 6). In addition to the early flares, the light curves of GRBs 050724 and 051221 exhibit evidence for delayed energy injection [22, 26], which may arise from extended engine activity and/or a wide distribution of ejecta Lorentz factors.

Given the short lifetime and dynamical timescale in the case of DNS or NS-BH mergers, the theoretical expectation is for simple afterglow evolution and a short duration of the γ -ray emission. The X-ray flares do not fit naturally in this scenario, although delayed activity arising from fragmentation of the accretion disk has been proposed and argued to agree with the basic observational signatures [40]. An intriguing alternative, in the context of accretion-induced collapse, is that the flares result from the interaction of the emerging blast wave with the giant companion star, with the timescale and duration of the flare set by the binary separation and the radius of the companion [10]. Two observations can be used to test this scenario: (i) multiple flares, and (ii) if most SHBs are collimated, then only the small fraction whose jets intercept the companion should exhibit flares.

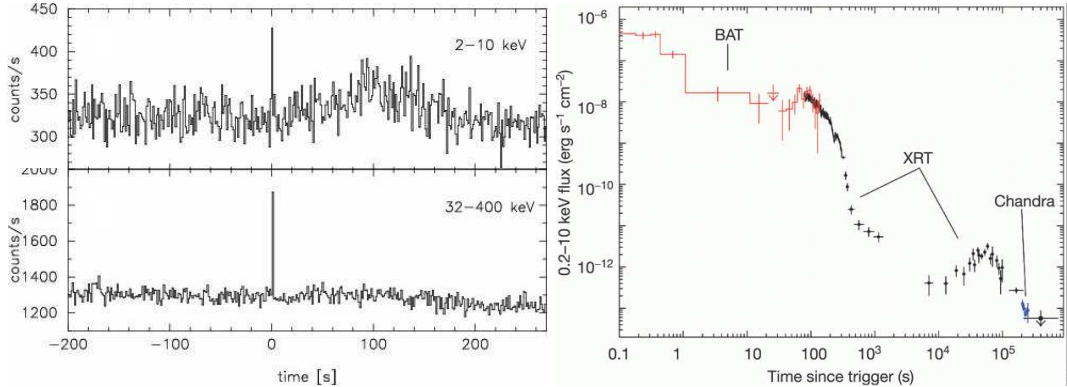


FIGURE 6. Flares in the prompt emission and X-ray afterglow of GRBs 050709 (left; Ref. [19]) and 050724 (right; Ref. [22]).

Host Galaxies and Offsets

One of the main clues that long GRBs are related to the death of massive stars came from their association with star forming galaxies. Long GRB hosts have star formation rates (SFR) typically in excess of $1 \text{ M}_\odot \text{ yr}^{-1}$ (and sometimes $> 100 \text{ M}_\odot \text{ yr}^{-1}$ [41]), stellar populations younger than $\sim 10^8 \text{ yr}$, and specific star formation rates that are higher than the general population of star forming galaxies [42]. In addition, the distribution of long GRBs relative to their hosts traces that of massive stars [43].

In a similar vein, we can use the hosts of SHBs to address the properties of the progenitors. The most striking difference compared to long GRBs is the existence of SHBs in elliptical galaxies. The limits on the SFR for the elliptical hosts of GRBs 050509b and 050724 are < 0.1 and $< 0.05 \text{ M}_\odot \text{ yr}^{-1}$, respectively [14, 18]. Even the star forming hosts of GRBs 050709 and 051221, with ~ 0.5 and $\sim 1.5 \text{ M}_\odot \text{ yr}^{-1}$, respectively, have lower SFRs than the median for hosts of long GRBs [20, 26]. The host of GRB 051221, moreover, exhibits evidence for an evolved stellar population and a near solar metallicity.

The mix of host types is reminiscent of type Ia supernovae (SNe Ia), which occur in both early- and late-type galaxies. It is interesting to note that the luminosity of SNe Ia is correlated with the host type, with intrinsically dimmer events occurring in early-type galaxies [44]. The current sample of SHBs is too small to address possible correlations of the burst and host properties, but this should become possible in the future.

It has also been noted that some SHBs occur in galaxy clusters. GRB 050509b is likely located in the cluster ZwCl 1234.0+02916, while GRB 050813 is most likely associated with a high redshift cluster. Several other cluster associations have been claimed for SHBs that lack arcsecond positions. At the present it is difficult to assess whether the latter associations are in fact correct, but some caution should be exercised given that the probability of finding a cluster in the NED archive within $10'$ from a random position on the sky is non-negligible, $\sim 5\%$ [45]. Moreover, since none of the SHBs with arcsecond positions are located in clusters, we consider the cluster associations claimed to date to be suggestive, though not secure.

Finally, as in the case of long GRBs the offset distribution has been proposed as

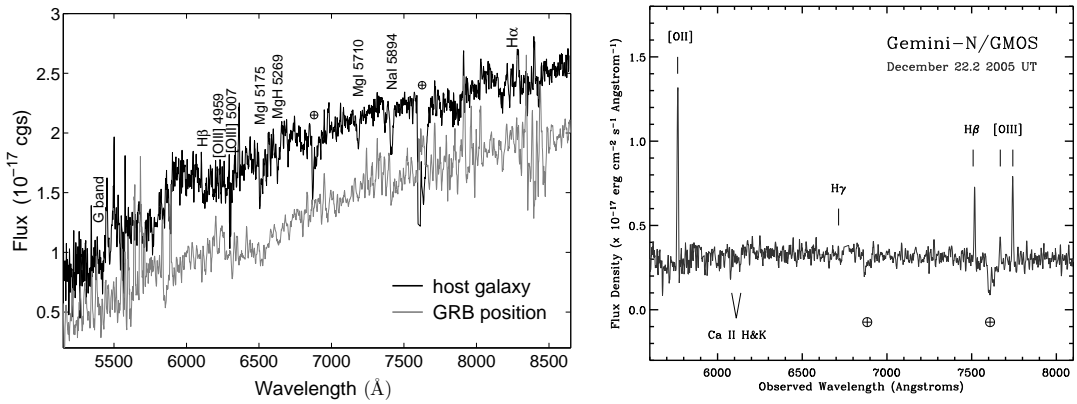


FIGURE 7. Spectra of the host galaxies of GRB 050724 (left) exhibiting typical features of an early-type galaxy, and GRB 051221 (right) exhibiting emission lines typical of star forming galaxies. From Refs. [18, 26].

a test of the progenitor population. The observed offsets in the coalescence model are a function of progenitor lifetimes, velocity kicks, and galaxy masses. Predictions from population synthesis models vary considerably, with possibly 50% of the bursts predicted to occur at offsets of > 10 kpc [11, 46]. Observationally, the offsets appear to be relatively small, \lesssim few kpc [18, 20, 26], but we stress that given the uncertain input distributions, this test may not be as useful as originally envisioned.

Event Rates and Progenitor Lifetimes

Another set of useful constraints on SHB models may be obtained from the event rates and the lifetime of the progenitors. Several authors have attempted to constrain the progenitor lifetime distribution using the BATSE flux distribution and the observed redshifts, leading to conflicting results. The canonical time delay distribution, $P(\tau) \propto 1/\tau$ as inferred from Galactic DNS systems, may be disfavored by the relatively low redshifts of some SHBs [47, 48], but is not ruled out [49]. Other lifetime distributions (with a constant delay or constant rate) also provide adequate fits. The redshift distribution, particularly when augmented by claimed associations for IPN SHBs [47], has been used to argue for lifetimes of ~ 6 Gyr with a relatively small spread [48]. We caution here that the IPN associations may be spurious¹ and in particular bias the result to longer lifetimes. Moreover, with $z \approx 1.8$ for GRB 050813 the progenitor lifetime is constrained to be $\lesssim 3$ Gyr.

A more profitable approach may be to investigate the relative fraction of SHBs in early- and late-type galaxies. For SNe Ia, which are more prevalent in late-type galaxies, similar analyses have led to the conclusion that the progenitor lifetimes are $\tau \sim 1 - 3$ Gyr [50]. In the case of SHBs, several authors have argued that the fraction in early-type

¹ The “brightest galaxy” criterion clearly fails for some of the precisely localized SHBs.

galaxies is larger, and therefore the progenitors lifetimes are longer than for SNe Ia, i.e. $\gtrsim 3$ Gyr [47]. This analysis is highly uncertain at the present, however, since of the three precisely localized SHBs, two are in fact located in late-type galaxies.

Finally, the SHB local event rate is inferred to be at least $R \sim 10 \text{ Gpc}^{-3} \text{ yr}^{-1}$ based on the BATSE rate and the current redshift distribution [48, 49]. The true rate is likely higher due to beaming, introducing a correction of $f_b^{-1} \sim 10 - 100$ for typical angles of $8 - 25^\circ$. Another unknown correction is due to the low-luminosity cutoff, $R \propto L_{\min}^{-1}$.

SUMMARY AND FUTURE DIRECTIONS

The progress in our understanding of SHBs over the last several months has shifted the field from the realm of speculation to a quantitative study. The observations made to date have allowed us to determine some of the most important and basic properties:

- SHBs occur at cosmological distances with a relatively wide spread in redshift; a local population may contribute up to 20% of the BATSE sample.
- The energy scale is typically lower than that of long GRBs, ranging from few $\times 10^{48}$ erg to $\gtrsim 10^{50}$ erg.
- The ejecta appear to be collimated, but with opening angles that are larger than the median for long GRBs.
- SHBs tend to occur in lower density environments than long GRBs.
- SHBs occur in elliptical and star forming galaxies, with roughly equal numbers.

These properties are in broad agreement with the DNS or NS-BH coalescence models, but other possibilities remain equally viable. In particular the observed long-term flares and injection episodes, as well as the spread in energies and host types, may point to multiple progenitor systems and/or energy extraction mechanisms. Clearly, an increased sample of events will shed additional light on the progenitor population. Future tests may include studies of the correlation between burst and host properties, evolution of the burst properties as a function of redshift, and perhaps the detection of gravitational waves in coincidence with an SHB. An intriguing possibility if SHBs in fact tend to be associated with galaxy clusters is that they may provide a beacon to select clusters at high redshift, $z \gtrsim 1.5$, where blind searches are exceedingly difficult. This may already be the case with GRB 050813.

ACKNOWLEDGMENTS

It is a pleasure to thank my collaborators for their hard work in pursuit of an understanding of short GRBs, in particular Derek Fox, Dale Frail, Mike Gladders, Shri Kulkarni, and Alicia Soderberg. This work was supported by a Hubble Post-doctoral Fellowship grant, HST-HF-01171.01.

REFERENCES

1. Strong, I. B., et al. *ApJ* **188**, L1 (1974).
2. Kouveliotou, C., et al. *ApJ* **413**, L101 (1993).
3. Eichler, D., et al. *Nature* **340**, 126 (1989).
4. B. Paczynski, *AcA* **41**, 257 (1991).
5. Narayan, R., et al. *ApJ* **395**, L83 (1992).
6. L. M. Katz, J. I. & Canel, *ApJ* **471**, 915 (1996).
7. Rosswog, S., et al. *MNRAS* **345**, 1077 (2003).
8. R. C. Thompson, C. & Duncan, *MNRAS* **275**, 255 (1995).
9. Qin, B., et al. *ApJ* **494**, L57 (1998).
10. MacFadyen, A. I., et al. *astro-ph* **0510192** (2005).
11. Fryer, C., et al. *ApJ* **516**, 892 (1999).
12. Hurley, K., et al. *ApJ* **567**, 447 (2002).
13. Gehrels, N., et al. *Nature* **437**, 851 (2005).
14. Bloom, J. S., et al. *astro-ph* **0505480** (2005).
15. Hjorth, J., et al. *ApJL* **630**, L117 (2005).
16. D. A. Soderberg, A. M. & Frail, *GCN* **3387** (2005).
17. Pedersen, K., et al. *ApJ* **634**, L17 (2005).
18. Berger, E., et al. *Nature* **438**, 988 (2005).
19. Villasenor, J. S., et al. *Nature* **437**, 855 (2005).
20. Fox, D. B., et al. *Nature* **437**, 845 (2005).
21. Hjorth, J., et al. *Nature* **437**, 859 (2005).
22. Barthelmy, S., et al. *Nature* **438**, 994 (2005).
23. E. Berger, *GCN* **3801** (2005).
24. Foley, R. J., et al. *GCN* **3801** (2005).
25. Gladders, M., et al. *GCN* **3798** (2005).
26. Soderberg, A. M., et al. *astro-ph* **0601455** (2006).
27. Parsons, A., et al. *GCN* **4363** (2005).
28. Golenetskii, S., et al. *GCN* **4394** (2005).
29. Burrows, D. N., et al. *GCN* **4366** (2005).
30. Tanvir, N., et al. *Nature* **438**, 991 (2005).
31. E. Freedman, D. L. & Waxman, *ApJ* **547**, 922 (2001).
32. Berger, E., et al. *ApJ* **590**, 379 (2003).
33. Sari, R., et al. *ApJ* **497**, L17 (1998).
34. Frail, D. A., et al. *ApJ* **562**, L55 (2001).
35. Bloom, J. S., et al. *ApJ* **594**, 674 (2003).
36. Berger, E., et al. *Nature* **426**, 154 (2003).
37. E. Li, W. H. & Ramirez-Ruiz, *ApJ* **577**, 893 (2002).
38. Lazatti, D., et al. *A&A* **379**, L39 (2001).
39. Connaughton, V., et al. *ApJ* **567**, 1028 (2002).
40. Perna, R., et al. *ApJ* **636**, L29 (2006).
41. Berger, E., et al. *ApJ* **588**, 99 (2003).
42. Christensen, L., et al. *A&A* **425**, 913 (2004).
43. Bloom, J. S., et al. *AJ* **123**, 1111 (2002).
44. Hamuy, M., et al. *AJ* **120**, 1479 (2000).
45. E. O. Ofek, *GCN* **4553** (2006).
46. K. Perna, R. & Belczynski, *ApJ* **570**, 252 (2002).
47. Gal-Yam, A., et al. *astro-ph* **0509891** (2005).
48. Nakar, E., et al. *astro-ph* **0511254** (2005).
49. T. Guetta, D. & Piran, *A&A* **435**, 421 (2002).
50. Tonry, J. L., et al. *ApJ* **594**, 1 (2003).